

Quark-antiquark spectroscopy and asymptotic freedom

Stefan Schmitz, Dana Beavis,* and Peter Kaus

Department of Physics, University of California, Riverside, California 92521

(Received 6 September 1985)

The $c\bar{c}$ and $b\bar{b}$ spectra are used to restrict the parameters of a QCD-inspired linear plus Coulomb potential. The potential incorporates a running coupling constant $\alpha(r)$, which is controlled by a parameter b . This parameter is virtually undetermined by the $c\bar{c}$ and $b\bar{b}$ spectra. The spectra are extrapolated to the $t\bar{t}$ regime for a variety of acceptable potentials or b values. It is shown how minimal $t\bar{t}$ measurements will restrict $\alpha(r)$ and determine $\Lambda_{\overline{\text{MS}}}$ (where $\overline{\text{MS}}$ denotes the modified minimal-subtraction scheme).

I. INTRODUCTION

The Ψ and Υ families of narrow resonances have been interpreted for the last ten years as bound states of the c and b quarks, respectively. For recent reviews see Refs. 1–5. The spectroscopy of these states has been very successfully tested by potential models with or without relativistic corrections. Successful potentials have been obtained by an inverse scattering method,⁶ by inspiration from QCD (Refs. 7–13), or pure phenomenology.^{14,15}

It is well known that $c\bar{c}$ and $b\bar{b}$ spectroscopies do not probe the potential at short distance, that is, shorter than ~ 0.1 fm (Refs. 12 and 16). This makes a variety of functional forms (ranging from single power,¹⁵ Coulomb plus linear^{7,12} to logarithmic at short distance, linear at large distance^{10,11}) equally successful in matching $c\bar{c}$ and $b\bar{b}$ data. The potentials of these models are essentially identical at distances larger than 0.1 fm, but at shorter distances there are marked differences. In a recent paper,¹⁷ Moxhay and Rosner compare the predictions of various models for $t\bar{t}$ spectroscopy by extrapolating to probable t -quark masses and find significant differences.

Here we take the approach of a single potential,¹¹ flexible enough to reproduce a whole range of differing small-distance behaviors, each interpreted as a different approach to asymptotic freedom and ultimately related to the QCD scale parameter $\Lambda_{\overline{\text{MS}}}$ (where $\overline{\text{MS}}$ denotes the modified minimal-subtraction scheme). Even limited information on $t\bar{t}$ spectroscopy will restrict the parameter b that controls the small-distance behavior of the potential and the value of $\Lambda_{\overline{\text{MS}}}$.

II. THE RUNNING COUPLING CONSTANT AND THE $q\bar{q}$ POTENTIAL

The form for the running coupling constant $\alpha(r)$ is suggested by a Fourier transform of the asymptotic-freedom result for $\alpha(q^2)$ which, for large momentum transfers, behaves as

$$\alpha(q^2) \rightarrow \left[\frac{12\pi}{33-2n_f} \right] \frac{1}{\ln(-q^2/\Lambda^2)}, \quad -q^2 \gg \Lambda^2. \quad (1)$$

Hence, $\alpha(r)$ has the following small-distance behavior:¹⁸

$$\alpha(r) \rightarrow \left[\frac{4\pi}{9} \right] \frac{1}{\ln[1/(\Lambda^2 e^{2\gamma} r^2)]}, \quad r \ll (\Lambda e^\gamma)^{-1}. \quad (2)$$

This form of $\alpha(r)$, however, has a singularity at $r = (\Lambda e^\gamma)^{-1}$ or in the neighborhood of 0.2–1 fm. Various modifications have been suggested, which may be considered as more or less arbitrary summations of a series with (1) or (2) as the leading large- q^2 (Ref. 10) or small- r^2 (Ref. 11) term.

The form chosen by Beavis, Chu, Desai, and Kaus¹¹ is given by

$$\alpha(r) = \left[\frac{4\pi}{9} \right] \frac{a}{\ln[b + 1/(\Lambda_0^2 e^{2\gamma} r^2)]}, \quad b > 1, \quad (3)$$

with $\Lambda_0 = 2.5 \text{ fm}^{-1}$ or 500 MeV. This potential has the transparent feature of interpolating between the asymptotic-freedom limit and intermediate radii which seem to be so well represented by a nonrunning Coulomb potential. The scale Λ_0 should not be confused with the QCD scale $\Lambda_{\overline{\text{MS}}}$. Λ_0 is merely a parameter of the running coupling constant $\alpha(r)$ and, through $r_\Lambda \equiv (\Lambda_0 e^\gamma)^{-1} \approx 0.22$ fm, is probably more related to the transition from a spherical cavity to a flux-tube regime. It is the combination of Λ_0 and the parameter b in Eq. (3) which is related to perturbative QCD and its scale $\Lambda_{\overline{\text{MS}}}$. This will be discussed in Sec. IV. The argument of the logarithm in Eq. (3) is $b + r_\Lambda^2/r^2$ and we can say

$$r^2 \gg \frac{r_\Lambda^2}{b} \quad \text{Coulomb},$$

$$r^2 \ll \frac{r_\Lambda^2}{b} \quad \text{asymptotic freedom}.$$

The low limit of b ($b = 1$) represents a configuration-space analog of the Richardson potential.¹⁰

The calculations of the quarkonia spectra in the next section were performed numerically using the potential of Beavis, Chu, Desai, and Kaus:¹¹

$$V(r) = -\frac{4}{3} \frac{\alpha(r)}{r} + (g_S + g_V)r + V_0, \quad (4)$$

where $\alpha(r)$ is given by Eq. (3). The couplings g_S and g_V refer to the usual scalar and vector couplings.

The relativistic corrections to the potential (4) were included in standard form¹⁹ as first-order perturbations. The spin-independent corrections are

$$V_{SI} = \frac{1}{M_Q^2} \left[\frac{2}{3r^3} [-2\alpha(r) + 2r\alpha'(r) - r^2\alpha''(r)] \mathbf{r} \cdot \nabla - \frac{\mathbf{P}^4}{4M_Q} + \frac{2}{3r} [2\alpha(r) - r\alpha'(r)] \nabla^2 - \frac{1}{3r} [2\alpha''(r) + \frac{1}{2}r\alpha'''(r)] + \frac{2}{3r^3} [\alpha(r) - r\alpha'(r)] l(l+1) + \frac{1}{2r} (g_V - g_S) [l(l+1) + 2] \right] \quad (5)$$

and the spin-dependent ones

$$V_{SD} = \frac{1}{M_Q^2} \left[\frac{1}{9r^3} [3\alpha(r) - 3r\alpha'(r) + r^2\alpha''(r)] S_{12} + \frac{1}{12r} g_V S_{12} - \frac{8}{9r} \alpha''(r) \mathbf{S}_1 \cdot \mathbf{S}_2 + \frac{4}{3r} g_V \mathbf{S}_1 \cdot \mathbf{S}_2 + \frac{2}{r^3} [\alpha(r) - r\alpha'(r)] \mathbf{L} \cdot \mathbf{S} + \frac{1}{2r} (3g_V - g_S) \mathbf{L} \cdot \mathbf{S} \right]. \quad (6)$$

III. $q\bar{q}$ POTENTIAL PARAMETERS, ASYMPTOTIC FREEDOM, AND t QUARKONIUM

The sensitivity of charmonium and the Υ system to asymptotic freedom was determined by variation of the parameter b in Eq. (3). The other parameters a , g_V , g_S , V_0 , m_c , and m_b were reevaluated by obtaining a best fit to the six lower lying charmonium and eight lower Υ states. We avoided the higher states, since we deemed them too close to the (four-quark) continuum and not as suitable to fix the parameters of the central potential. Tables I–III contain the parameters, levels, and ratios of leptonic widths obtained by the fits. The parameters g_V , g_S , V_0 , m_c , and m_b are shown as functions of b in Figs. 1–3, as well as the overall figure of merit.

Acceptable fits were found in the interval from $b=4$ to $b=10^4$ (essentially Coulomb, i.e., $b=\infty$). The best fit was $b=20$, but no significance can be attached to this, since the rms error for this fit ($b=20$) was 0.2%, while in the entire range, $b=4$ to $b=10^4$, the error was never larger than 0.4%. Thus the $c\bar{c}$ and $b\bar{b}$ spectra are not sensitive to the incorporation of asymptotic freedom in the potential excluding only the range $b < 4$ in our potential. Figure 4 compares the best fit ($b=20$) with experimental $q\bar{q}$ masses.

The running coupling constant as a function of b for $r=\infty$, $r=r_\Lambda$, and $r=r_\Lambda/10$ is shown in Fig. 5. As b is decreased the reevaluation of the parameter a causes the value of $\alpha(\infty)$ and $\alpha(r_\Lambda)$ to increase; however $\alpha(r_\Lambda/10)$ decreases. The ratio $\alpha(r)/\alpha(\infty)$ which removes the effects of a is shown in Fig. 6.

For the entire range of acceptable b 's, g_V and g_S are about equal and their sum is 1.2–1.3 GeV/fm. The 3P_J level splittings are particularly sensitive to the g_V/g_S ratio. The ratios $R \equiv ({}^3P_2 - {}^3P_1) / ({}^3P_1 - {}^3P_0)$ for the χ_c , χ_b , and χ'_b states are given by experiment²⁰ as 0.48, 0.93, and 0.83, respectively. Our fit which was only concerned with fitting energy levels gives $R=0.91$, 0.90, and 0.88. The $g_V \approx g_S$ result is an artifact of the potential form and more parameters in the central potential $V(r)$ could replace the vector presence in the confining potential $(g_V + g_S)r$.

In Fig. 7 we show the potential [Eq. (4)] as a function of r for $b=6, 20, 100, 10^4$. On the graph we indicate the rms radii and expectation values of the central potential for the $1S$ states of the charm, bottom, and top systems (assuming $m_t=40$ GeV) for the various b values. Here we see that the charm and bottom systems probe distances that are essentially not effected by asymptotic freedom. Although the hyperfine splittings probe smaller values of r they do not give sufficient sensitivity to the parameter b because of compensations among the other potential parameters.

The independence of the spectrum on the assumptions about the r dependence of $\alpha(r)$ ceases drastically when the calculation is extrapolated to quark masses in the probable top-quark region (40–50 GeV). The $2S$ - $1S$ and $3S$ - $1S$ excitation energies are shown in Table IV and Figs. 8(a) and 8(b). As we discussed previously,¹¹ the quark-mass independence of the excitation spectrum for charmonium and Υ is in no way fundamental and we are not surprised that when the larger quark masses produce bound states, large deviations result. The potential is now

TABLE I. The potential parameters and the rms error for the various values of b .

b	a	g_V (GeV/fm)	g_S (GeV/fm)	V_0 (GeV)	m_c (GeV)	m_b (GeV)	Error (%)
2	0.3975	0.7656	0.5922	-0.9954	1.921	5.272	0.6124
4	0.5348	0.6593	0.5118	-0.9818	1.919	5.274	0.3696
6	0.6263	0.5945	0.5207	-0.9979	1.924	5.280	0.2804
10	0.6410	0.5674	0.6423	-1.046	1.903	5.261	0.2447
20	0.7679	0.5718	0.6194	-1.047	1.899	5.258	0.2169
10^2	0.9910	0.6720	0.5848	-1.074	1.870	5.235	0.2576
10^3	1.342	0.7396	0.5687	-1.107	1.860	5.226	0.2962
10^4	1.801	0.7627	0.5380	-1.130	1.874	5.240	0.3026

TABLE II. The calculated energy levels of the 14 states used in the fits for the various values of b and the experimental results in units of GeV with b dimensionless.

b	η_c	J/ψ	$c\bar{c}$ system			ψ'
			(1^3P_0)	(1^3P_1)	(1^3P_2)	
2	3.005	3.096	3.392	3.467	3.553	3.726
4	2.991	3.103	3.396	3.481	3.568	3.701
6	2.984	3.107	3.403	3.488	3.570	3.692
10	2.986	3.102	3.410	3.488	3.560	3.697
20	2.982	3.107	3.412	3.490	3.561	3.692
10^2	2.981	3.110	3.408	2.487	3.561	3.697
10^3	2.983	3.110	3.405	3.484	3.561	3.702
10^4	2.981	3.112	3.404	3.484	3.562	3.700
Expt ^a	2.981 ± 0.006	3.0969 ± 0.0001	3.4150 ± 0.0010	3.5100 ± 0.0006	3.5558 ± 0.0006	3.6860 ± 0.0001

b	Υ	$b\bar{b}$ system						
		(1^3P_0)	(1^3P_1)	(1^3P_2)	Υ'	(2^3P_0)	(2^3P_1)	(2^3P_2)
2	9.508	9.822	9.840	9.860	10.047	10.268	10.281	10.296
4	9.482	9.835	9.862	9.889	10.038	10.254	10.273	10.292
6	9.468	9.842	9.872	9.902	10.034	10.249	10.271	10.292
10	9.467	9.844	9.874	9.900	10.029	10.250	10.272	10.292
20	9.461	9.849	9.880	9.908	10.023	10.245	10.270	10.292
10^2	9.468	9.851	9.882	9.909	10.020	10.246	10.271	10.294
10^3	9.475	9.848	9.877	9.903	10.018	10.244	10.269	10.291
10^4	9.475	9.848	9.878	9.904	10.018	10.243	10.269	10.291
Expt ^a	9.4600 ± 0.0003	9.8729 ± 0.0058	9.8945 ± 0.0035	9.9146 ± 0.0024	10.0234 ± 0.0003	10.2328 ± 0.0058	10.2537 ± 0.0034	10.2710 ± 0.0024

^aParticle Data Group, Ref. 20.

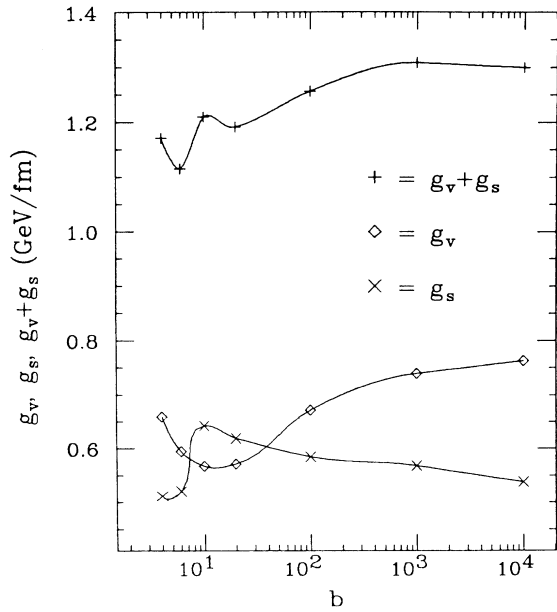


FIG. 1. The vector and scalar coupling constants of the linear confining potential, g_v and g_s , and their sum as functions of b .

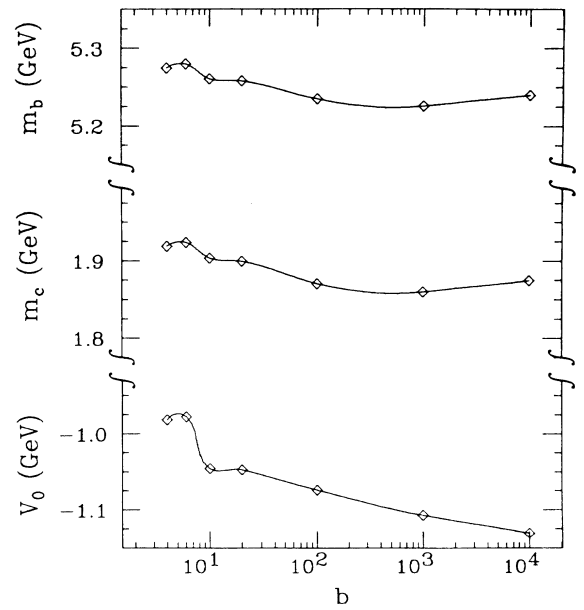


FIG. 2. The quark masses m_b and m_c and the constant V_0 as functions of b .

TABLE III. Ratios of leptonic widths, $\Gamma_{ee}(2S)/\Gamma_{ee}(1S)$, for the various values of b and the experimental results. In potential theory the leptonic width is given by the Weisskopf-Van Royen formula [R. Van Royen and V. F. Weisskopf, *Nuovo Cimento* **50**, 617 (1967)]: $\Gamma_{ee}(nS) = 16\pi e_Q^2 \alpha^2 |\psi(0)|^2 / M_n^2$. However, radiative and relativistic corrections to this result are very large. They cancel partially in the ratios. Buchmüller and Tye (Ref. 12) estimate the uncertainties for the ratios to be about 30% in the case of charmonium and about half of that in the case of Υ . The calculations for the top system were done assuming $m_t = 40$ GeV.

b	$c\bar{c}$	$b\bar{b}$	$t\bar{t}$
2	0.58	0.76	0.67
4	0.50	0.57	0.52
6	0.48	0.51	0.44
10	0.50	0.51	0.40
20	0.50	0.48	0.32
10^2	0.52	0.49	0.23
10^3	0.54	0.51	0.19
10^4	0.54	0.51	0.18
Expt ^a	0.45 ± 0.06	0.42 ± 0.04	

^aParticle Data Group, Ref. 20.

probed at $r < r_\Lambda \approx 0.2$ fm and the parameter b , which heralds the onset of asymptotic freedom becomes important. Υ , where the $2S$ - $1S$ excitation energy is about 0.56 GeV, was fit by the parameter b varying from $b=4$ to $b=10^4$, with a spread of about 0.02 GeV. At a t -quark mass of 40 GeV these potentials could give for the $2S$ - $1S$

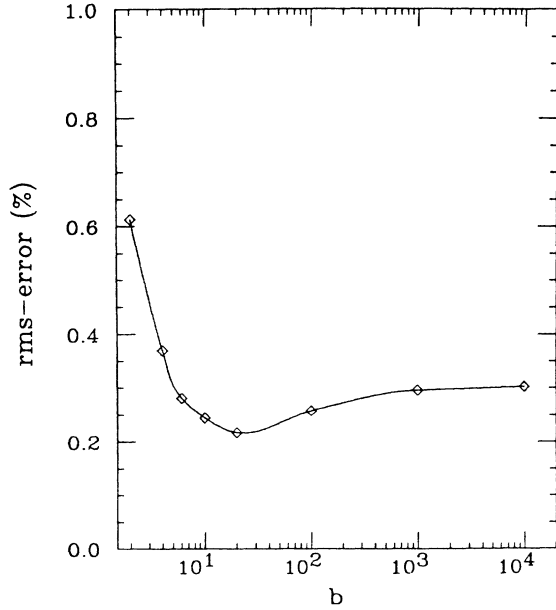


FIG. 3. The root-mean-square error of the fit (in %) as a function of b . The rms error is defined as

$$\left[\frac{1}{14} \sum_{i=1}^{14} \left(\frac{m_i^{\text{calc}} - m_i^{\text{expt}}}{m_i^{\text{expt}}} \right)^2 \right]^{1/2}$$

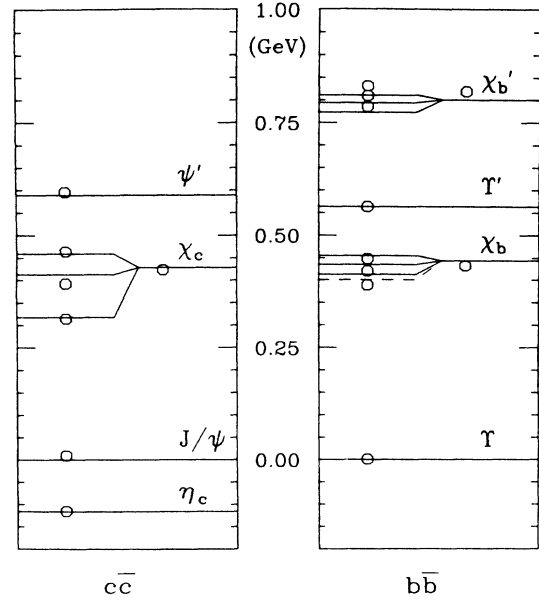


FIG. 4. The experimental (Ref. 20) (solid lines) and calculated (circles) values of the energy levels with respect to J/ψ and Υ . Shown are the 14 states in the fits and the centers of gravity for the triplet- p states. According to the Crystal Ball Collaboration (Ref. 27) the $\chi_b(^3P_0)$ state is moved to the dashed line. This figure represents the best overall fit with $b=20$ and an rms error of 0.22%.

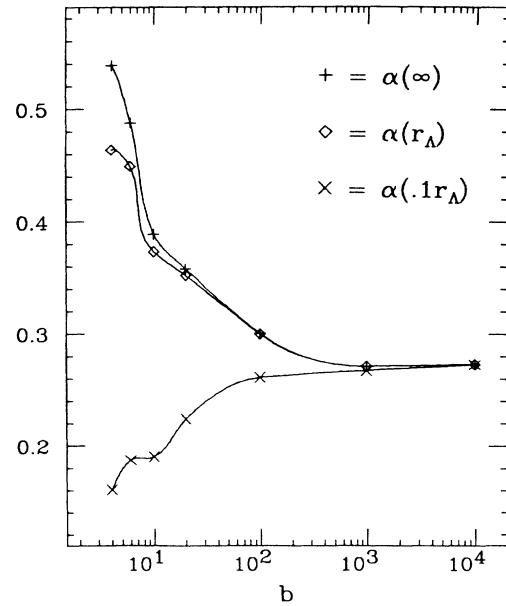


FIG. 5. The running coupling constant α as a function of the parameter b for three radii, $r = \infty$, $r = r_\Lambda \approx 0.2$ fm, and $r = r_\Lambda/10$.

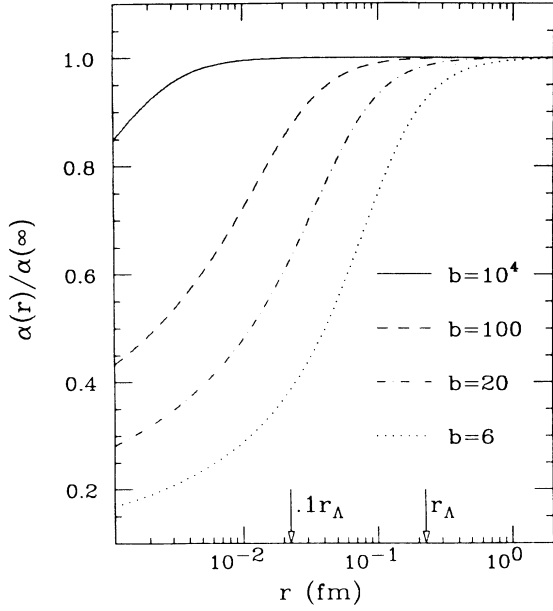


FIG. 6. The ratio $\alpha(r)/\alpha(\infty)$ as a function of r for four values of b ($b=6, 20, 100, 10^4$).

excitation energy a value from 0.49 GeV ($b=4$) to 1.15 GeV ($b=10^4$). Thus the minimal measurement of the nS - $1S$ splittings will be quite sensitive to asymptotic freedom in the potential.

In a recent article¹⁷ Moxhay and Rosner compare the properties of various models^{12,13,15,21} for $m_t=40$ GeV.

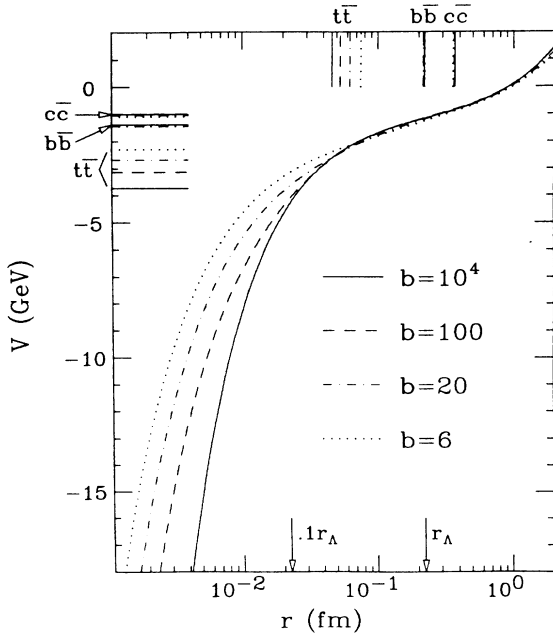


FIG. 7. The potential as a function of r for four values of b ($b=6, 20, 100, 10^4$). The marks show the rms radii (top edge) and expectation values of the central potential (left edge) for the $1S$ states of $c\bar{c}$, $b\bar{b}$, and $t\bar{t}$ (assuming $m_t=40$ GeV) for the above-mentioned values of b .

We find that the model potential used here, Eq. (4), which interpolates, through the parameter b of Eq. (3), from Coulombic (large b) to “normal” asymptotic freedom (small b), interpolates between various models as well. Thus $b=100$ closely matches the results of Moxhay and Rosner²¹ for $t\bar{t}$ excitation energies, $b=70$ those of Kühn

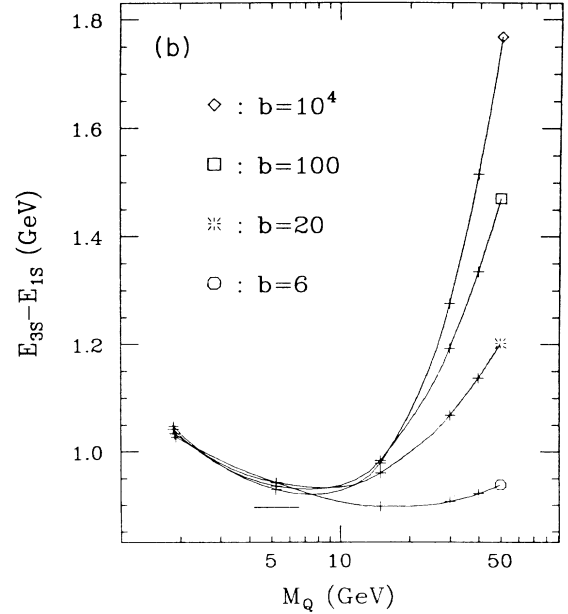
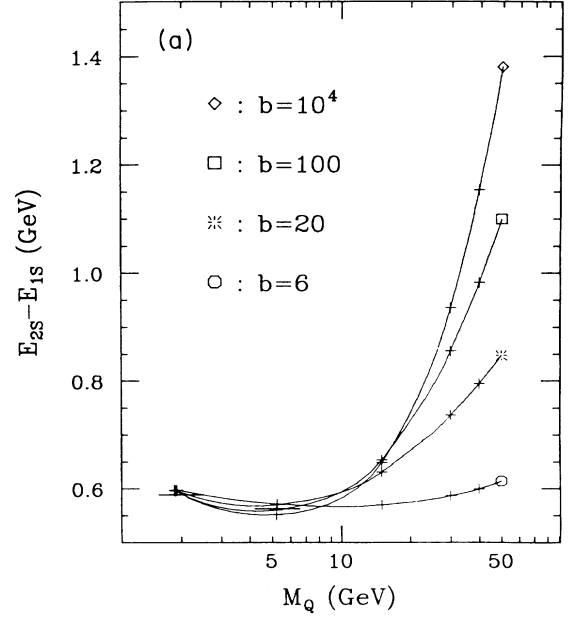


FIG. 8. The excitation energies (a) $E_{2S}-E_{1S}$ and (b) $E_{3S}-E_{1S}$ as functions of the quark mass for four values of b ($b=6, 20, 100, 10^4$). Here E_{nS} is the center of gravity of the singlet and triplet states. The points close to $m_Q=2$ and 5 GeV correspond to the $c\bar{c}$ and $b\bar{b}$ systems, respectively. The horizontal bars represent experimental values (Ref. 20).

TABLE IV. The ground-state and excitation energies of the nS states for $t\bar{t}$ (assuming $m_t=40$ GeV) for the various values of b in units of GeV with b dimensionless. The energies E_{nS} are the centers of gravity of the singlet and triplet states.

b	E_{1S}	$E_{2S}-E_{1S}$	$E_{3S}-E_{1S}$
2	78.513	0.341	0.596
4	78.297	0.494	0.791
6	78.147	0.600	0.921
10	78.123	0.651	0.974
20	77.949	0.796	1.138
10^2	77.772	0.983	1.336
10^3	77.676	1.078	1.432
10^4	77.555	1.154	1.517

and Ono¹³ (model b , the Richardson potential), $b=40$ corresponds to Buchmüller and Tye¹² (for $\Lambda_{\overline{MS}}=500$ MeV), $b=9$ to Kühn and Ono¹³ (model a , the T potential), $b=7$ to Buchmüller and Tye¹² (for $\Lambda_{\overline{MS}}=200$ MeV), and finally $b=4$ to Martin.¹⁵

IV. THE RUNNING COUPLING CONSTANT, t QUARKONIUM, AND $\Lambda_{\overline{MS}}$

The discussion is entirely in the context of the potential (4) in which the phenomenological running coupling constant is given by (3)

$$\alpha(r) = \left[\frac{4\pi}{9} \right] \frac{a}{\ln(b + r_\Lambda^2/r^2)}$$

with $r_\Lambda \equiv (\Lambda_0 e^\gamma)^{-1} \approx 0.22$ fm or $\Lambda_0=500$ MeV.

We find that the $c\bar{c}$ and $b\bar{b}$ spectrum does not strongly constrain the parameter b . However, while the inclusion of asymptotic freedom through the logarithmic term in $\alpha(r)$ cannot do much good (Fig. 3), it can do considerable harm for $b < 4$. The phenomenology of $c\bar{c}$ and $b\bar{b}$ spectroscopy probes the potential down to $r \approx 0.2$ fm and demands that the running coupling constant be greater than 80% of its asymptotic value at $r=0.2$ fm, i.e., $\alpha(0.2)/\alpha(\infty) > 0.8$. Since $\alpha(0.2)/\alpha(\infty) \approx \ln(b)/\ln(b+1)$ this translates into $b \geq 4$ in our potential. On the other hand, $t\bar{t}$ spectroscopy with $m_t \approx 40$ GeV will be sensitive

to the potential to ~ 0.05 fm and will certainly determine b to one significant figure (Fig. 8, Table IV).

The restriction $b \geq 4$ does have significance for perturbative QCD. We matched the phenomenological $\alpha(r\Lambda_0, b)$, Eq. (3), with the running coupling constant, $\alpha(r\Lambda_{\overline{MS}})$, obtained from perturbative QCD (Ref. 12). This was done at several values of $\rho \equiv r\Lambda_{\overline{MS}}$, ranging from $\frac{1}{20}$ to $\frac{1}{50}$. The results are shown in Table V along with the matching radii.

We see from this exercise that the Λ_0 of our own $\alpha(r)$, which corresponds to a critical distance $r_\Lambda \approx 0.22$ fm is not simply related to $\Lambda_{\overline{MS}}$. Rather we may think of r_Λ/b as a measure of the radius where a transition from the flux-tube-string regime to the perturbative regime occurs. The running coupling constant $\alpha(r)$ in the neighborhood of r_Λ/b changes from the perturbative QCD prescription $\alpha(r\Lambda_{\overline{MS}})$ to perhaps the string prescription $\alpha \approx (\frac{3}{4})\pi/12$ (Ref. 22). In any case the matching to a perturbative QCD potential $\alpha(r\Lambda_{\overline{MS}})$ should be done at $r = \rho/\Lambda_{\overline{MS}} \lesssim r_\Lambda/b$. From Table V we see that this condition is met by $\rho = \frac{1}{20}$ or smaller, which should also be small enough for perturbative QCD to converge well. The fact that for the best fits, $b \approx 20$, $\Lambda_{\overline{MS}}$ does not change much with the fitting radius $\rho/\Lambda_{\overline{MS}}$, shows that our phenomenological $\alpha(r)$ blends well into the perturbative $\alpha(r\Lambda_{\overline{MS}})$. Thus, the condition $b \geq 4$ would seem to indicate that $\Lambda_{\overline{MS}} \geq 120$ MeV. The best fit, $b=20$, gives an $\alpha(r)$ which fits very smoothly into a perturbative $\alpha(r\Lambda_{\overline{MS}})$ with $\Lambda_{\overline{MS}}=240$ MeV. This should dispell the notion that $c\bar{c}$ and $b\bar{b}$ phenomenology demands a $\Lambda_{\overline{MS}}$ greater than 300 MeV. A compilation of $\Lambda_{\overline{MS}}$ determinations shows that $\Lambda_{\overline{MS}} \approx 200$ MeV may not be inconsistent with most considerations²³ and it is certainly not inconsistent with ours, putting b somewhere in the range of $b=10-20$. In this range we also agree well with t -quarkonium predictions of Clavelli, Lichtenberg, and Willis.²⁴

The importance of the t -quarkonium spectrum then lies in the fact that this consistency can well be destroyed by almost any information on the excitation spectrum. For example, taking a hypothetical top-quark mass of 40 GeV, we see from Table IV, that if the $2S-1S$ excitation energy is larger than 800 MeV, b is larger than 20 and $\Lambda_{\overline{MS}}$ larger than 240 MeV. Conversely, if $2S-1S$ is smaller

TABLE V. The QCD scale parameter $\Lambda_{\overline{MS}}$ and the matching radius r for each b . The values are obtained by matching the phenomenological coupling constant, $\alpha(r\Lambda_0, b)$, and the perturbative QCD coupling constant (using $n_f=4$, to second order in $[\ln(1/r^2\Lambda_{\overline{MS}}^2)]^{-1}$, according to Ref. 12) $\alpha(r\Lambda_{\overline{MS}})$, at a fixed $\rho = r\Lambda_{\overline{MS}}$. The table shows the results for four different values of ρ .

b	$\rho = \frac{1}{20}$	$\rho = \frac{1}{30}$	$\rho = \frac{1}{40}$	$\rho = \frac{1}{50}$
	$\Lambda_{\overline{MS}}(r)$ (MeV)(0.01 fm)	$\Lambda_{\overline{MS}}(r)$ (MeV)(0.01 fm)	$\Lambda_{\overline{MS}}(r)$ (MeV)(0.01 fm)	$\Lambda_{\overline{MS}}(r)$ (MeV)(0.01 fm)
2	100(9.5)	85(7.7)	70(6.7)	65(6.0)
4	150(6.7)	130(5.1)	120(4.2)	110(3.7)
6	190(5.3)	170(3.8)	160(3.1)	150(2.7)
10	180(5.6)	170(3.8)	160(3.1)	150(2.6)
20	240(4.1)	250(2.6)	250(2.0)	240(1.6)
100	330(3.0)	460(1.4)	500(0.98)	520(0.76)

than 500 MeV, then $b < 4$. This would imply that $\Lambda_{\overline{\text{MS}}} < 120$ MeV, which is pleasing to some determinations, but $b < 4$ gives a very poor fit to $c\bar{c}$ and $b\bar{b}$ spectra. Similar relationships for other excitation energies such as $3S$ - $1S$ as well as other top-quark masses can be obtained from Table IV and Figs. 8(a) and 8(b).

The phenomenological potential (4) does not agree with perturbative QCD as r vanishes. Any extraction of $\Lambda_{\overline{\text{MS}}}$, however, depends on consistency with QCD.

We have modified an expression by Buchmüller and Tye^{12,25} for the inverse β function, by adding a simple function which leaves intact the asymptotic properties at small and large Q , but alters the behavior in the transition region ($2 < Q < 20$ GeV) smoothly. In this manner, it was possible to find expressions for the Fourier transform of the potential, consistent with perturbative QCD and with the whole range of phenomenological potentials (4).

We found for each b an acceptable range of $\Lambda_{\overline{\text{MS}}}$:

$$\begin{aligned} b=2, & \quad \Lambda_{\overline{\text{MS}}} = 80 \pm 20 \text{ MeV}, \\ b=6, & \quad \Lambda_{\overline{\text{MS}}} = 150 \pm 50 \text{ MeV}, \\ b=20, & \quad \Lambda_{\overline{\text{MS}}} = 260 \pm 60 \text{ MeV}, \\ b=50, & \quad \Lambda_{\overline{\text{MS}}} = 400 \pm 100 \text{ MeV}, \\ b=100, & \quad \Lambda_{\overline{\text{MS}}} = 700 \pm 200 \text{ MeV}. \end{aligned}$$

The range of $\Lambda_{\overline{\text{MS}}}$ comes from the fact that the interpolating function has two parameters, which allows some range for the transition region. Limited by the demand for fitting the phenomenological potential at small Q and

blending smoothly into the perturbative expression at large Q , we found the transition region \overline{Q} for $b=2$ is $2 < \overline{Q} < 3$ GeV, while for $b=100$ acceptable potentials were found with $10 < \overline{Q} < 20$ GeV.

In conclusion, the $c\bar{c}$ and $b\bar{b}$ spectrum provides us with very little information about asymptotic freedom and its scale $\Lambda_{\overline{\text{MS}}}$. If we take $6 < b < 50$ as the range of “acceptable” potentials, then this implies $\Lambda_{\overline{\text{MS}}} = 300 \pm 200$ MeV. This is somewhat more pessimistic than an estimate by Hagiwara, Jacobs, and Olsson,²⁶ who obtain $\Lambda_{\overline{\text{MS}}} = 250 \pm 100$ MeV. The $t\bar{t}$ spectrum will certainly narrow the choice of b . This, in turn, will constrain $\Lambda_{\overline{\text{MS}}}$. For example, if $b=20$ remains the optimum b , we obtain $\Lambda_{\overline{\text{MS}}} = 260 \pm 60$ MeV, in good agreement with the expectations from the “fake” data of Hagiwara, Jacobs, and Olsson.²⁶ Should the higher b values, such as for example $b=100$, become more favorable from real t -quarkonium data, then $\Lambda_{\overline{\text{MS}}}$ would increase dramatically, but so would the uncertainty. It will be possible to bracket the scale of asymptotic freedom in $q\bar{q}$ spectroscopy, when there is some manifestation of the running coupling constant. However, if $b \gg 20$, that is larger t -quarkonium excitation energies, then even t quarkonium does not feel this effect.

ACKNOWLEDGMENTS

We wish to thank S. Meshkov, M. G. Olsson, and J. L. Rosner for fruitful discussions. This work was supported by the U.S. Department of Energy under Contract No. DE-AM03-76SF00034.

*Present address: Brookhaven National Laboratory, Upton, New York 11973.

¹K. Gottfried, in *Proceedings of HEP83*, International Europhysics Conference on High Energy Physics, Brighton, 1983, edited by J. Guy and C. Costain (Rutherford Laboratory, Chilton, England, 1983).

²E. Eichten, in *The Sixth Quark*, proceedings of the 12th SLAC Summer Institute on Particle Physics, Stanford, California, edited by P. M. McDonough (SLAC Report No. 281, SLAC, Stanford, 1985).

³J. L. Rosner, in *Experimental Meson Spectroscopy—1983* (Seventh International Conference, Brookhaven), proceedings, Upton, New York, 1983, edited by S. J. Lindenbaum (AIP Conf. Proc. No. 113) (AIP, New York, 1984).

⁴W. Buchmüller, in *Fundamental Interactions in Low Energy Systems*, proceedings of the Fourth Course of the International School of Physics of Exotic Atoms, Erice, Italy, 1984, edited by P. Dalpiaz, G. Fiorentini, and G. Torelli (Ettore Majorana International Science Series: Physical Sciences, Vol. 23) (Plenum, New York, 1985).

⁵J. L. Rosner, in *Proceedings of the Sixth International Symposium on High Energy Spin Physics*, Marseille, France, 1984, edited by J. Soffer [J. Phys. (Paris) Colloq. **46**, C2-77 (1985)].

⁶H. B. Thacker, C. Quigg, and J. L. Rosner, Phys. Rev. D **18**, 274 (1978); **18**, 287 (1978); **21**, 234 (1980); C. Quigg, and J. L. Rosner, *ibid.* **23**, 2625 (1981).

⁷E. Eichten, K. Gottfried, T. Kinoshita, K. D. Lane, and T. M. Yan, Phys. Rev. D **17**, 3090 (1978); **21**, 203 (1980).

⁸D. Beavis, S.-Y. Chu, B. R. Desai, and P. Kaus, Phys. Rev. D **20**, 743 (1979).

⁹R. Levine and Y. Tomozawa, Phys. Rev. D **19**, 1572 (1979).

¹⁰J. L. Richardson, Phys. Lett. **82B**, 272 (1979).

¹¹D. Beavis, S.-Y. Chu, B. R. Desai, and P. Kaus, Phys. Rev. D **20**, 2345 (1979).

¹²W. Buchmüller and S.-H. Tye, Phys. Rev. D **24**, 132 (1981).

¹³J. H. Kühn and S. Ono, Z. Phys. C **21**, 395 (1984); **24**, 404(E) (1984).

¹⁴C. Quigg and J. L. Rosner, Phys. Lett. **71B**, 153 (1977).

¹⁵A. Martin, Phys. Lett. **100B**, 511 (1981).

¹⁶See, for example, C. Quigg, Acta Phys. Pol. **B15**, 53 (1984).

¹⁷P. Moxhay and J. L. Rosner, Phys. Rev. D **31**, 1762 (1985).

¹⁸W. Celmaster, H. Georgi, and M. Machacek, Phys. Rev. D **17**, 879 (1978).

¹⁹H. J. Schnitzer, Phys. Rev. D **13**, 74 (1976); D. Gromes, Nucl. Phys. **B131**, 80 (1977); W. Celmaster and F. Henyey, Phys. Rev. D **17**, 3268 (1978).

²⁰Particle Data Group, Rev. Mod. Phys. **56**, S1 (1984).

²¹P. Moxhay and J. L. Rosner, Phys. Rev. D **28**, 1132 (1983).

²²M. Luscher, K. Symanzik, and P. Weisz, Nucl. Phys. **B173**, 365 (1980); J. D. Stack and M. Stone, Phys. Lett. **100B**, 476 (1981).

²³D. W. Duke and R. G. Roberts, Phys. Rep. **120**, 275 (1985).

- ²⁴L. Clavelli, D. B. Lichtenberg, and J. G. Wills, Phys. Rev. D **33**, 284 (1986).
- ²⁵The β function of Ref. 12 is, of course, process dependent; it is defined in terms of a particular physical quantity, the quark-antiquark potential. In this connection, see S. J. Brodsky, G. P. Lepage, and P. B. Mackenzie, Phys. Rev. D **28**, 228 (1983).
- ²⁶K. Hagiwara, S. Jacobs, and M. G. Olsson, Phys. Lett. **130B**, 209 (1983).
- ²⁷R. Nernst *et al.*, Phys. Rev. Lett. **54**, 2195 (1985).